



Effects of operating and design parameters on ion exchange columns for nutrient recovery from urine

Journal:	<i>Environmental Science: Water Research & Technology</i>
Manuscript ID	EW-ART-11-2017-000478.R1
Article Type:	Paper
Date Submitted by the Author:	23-Feb-2018
Complete List of Authors:	Tarpeh, William ; University of California Berkeley, Civil & Environmental Engineering Wald, Ileana; University of California Berkeley, Civil & Environmental Engineering Wiprächtiger, Maja; Sprachenzentrum der Universität und der ETH Zurich, Institute of Environmental Engineering Nelson, Kara; University of California Berkeley,

1
2
3
4
5
6
7
8
9
10
11
12
13
14
15
16
17
18
19
20
21
22
23
24
25
26
27
28
29
30
31
32
33
34
35
36
37

Effects of operating and design parameters on ion exchange columns for nutrient recovery from urine

William A. Tarpeh^{†#}, Ileana Wald^{†#}, Maja Wiprächtiger[‡], and Kara L. Nelson^{†#*}

[†]Department of Civil and Environmental Engineering, University of California, Berkeley, CA 94720, United States

[#]Engineering Research Center for Re-inventing the Nation’s Urban Water Infrastructure (ReNUWIt), United States

[‡]Institute of Environmental Engineering, ETH Zürich, Stefano-Franscini-Platz 5, CH-8093 Zürich, Switzerland

Submitted to:

Environmental Science: Water Research & Technology

*Corresponding author: karanelson@berkeley.edu

38 **ABSTRACT**

39 Ion exchange is a promising option for recovering nutrients (nitrogen, phosphorus, and
40 potassium) from source-separated urine. We determined that it was feasible to integrate nitrogen
41 and potassium recovery via cation exchange with phosphorus recovery, either via struvite
42 precipitation or anion exchange. Flow rate and intermittent operation did not significantly affect
43 ammonium recovery and adsorption kinetics with Dowex Mac 3, a resin with demonstrated high
44 adsorption density and recovery efficiency. During regeneration, concentration of the sulfuric
45 acid eluent had a more significant effect on performance metrics than did acid flow rate. Nitric
46 acid and hydrochloric acid exhibited similar cation recovery efficiencies as sulfuric acid (>99%);
47 sodium chloride, which has lower costs and environmental impacts associated with its
48 production, exhibited lower recovery efficiencies (77% for ammonium, 88% for potassium). A
49 suite of common pharmaceuticals was used to determine trace organic contaminant fate during
50 adsorption, regeneration, and in the final fertilizer product. Of the ten pharmaceuticals measured,
51 only atenolol and metoprolol were detected in the ammonium sulfate product, both at $<0.1 \mu\text{g L}^{-1}$.
52 Ultimately, macronutrients were selectively recovered from urine, which could enable
53 customized fertilizer production.

54

55 **Water Impact Statement**

56 Ion exchange was used to recover nitrogen, phosphorus, and potassium from urine. This
57 approach aims to remove nutrients at lower cost and energy than treating combined wastewater,
58 while also generating fertilizer. The process was robust over varying flow rates, influent
59 concentrations, and intermittent operation. These promising results provide a basis for evaluating
60 fertilizer production from urine at the pilot scale.

61 1. INTRODUCTION

62 Effluent from centralized wastewater treatment plants is a significant source of nutrients, which
63 contribute to the accelerated eutrophication of natural water bodies. Separate collection and
64 treatment of urine at the toilet is a potential alternative to biological nutrient removal at
65 wastewater treatment plants. Nutrients in urine can be removed and recovered to offset energy-
66 intensive synthetic fertilizers.¹ Furthermore, revenue generated from the sale of urine-derived
67 fertilizers could reduce the cost of excreta collection and treatment services. Nutrient recovery
68 from human urine has garnered increasing interest because urine contributes approximately 80%
69 of the nitrogen (N), 50% of the phosphorus (P), and 70% of the potassium (K) load in municipal
70 wastewater streams, but comprises only 1% of the liquid volume.²

71
72 Several techniques have emerged for recovering either nitrogen, phosphorus or potassium from
73 urine. Phosphorus is often recovered via precipitation of struvite ($\text{MgNH}_4\text{PO}_4 \cdot 6\text{H}_2\text{O}$), a slow-
74 release fertilizer.^{1,3,4} Anion exchange for phosphorus removal has also been explored.⁵ Nitrogen
75 has been recovered from urine using electrochemical separation,^{6,7} microbial electrochemical
76 approaches,^{8,9} and cation exchange.¹⁰ Thus far, potassium recovery has been preliminarily
77 explored in real urine with limited recovery¹² and in ideal salt solutions with clinoptilolite
78 membranes.¹³ These techniques can be combined to recover nitrogen and phosphorus, such as
79 struvite precipitation for phosphorus and cation exchange on zeolite for nitrogen.¹¹ Combining
80 treatment technologies into a full urine treatment train that recovers nitrogen, phosphorus, and
81 potassium is a logical next step. Ultimately, selective recovery of nitrogen, phosphorus, and
82 potassium could lead to tailored fertilizer production from urine.

83

84 Phosphorus recovery by struvite precipitation in urine has been well-characterized in terms of
85 magnesium dosage, mixing, and precipitation mechanisms.^{1,14,15} Similarly, equilibrium and
86 kinetic models have been developed for adsorption and regeneration of anion exchange resins.^{5,16}
87 In comparison, design and operating parameters have not been optimized for recovering nitrogen
88 from urine via cation exchange, although the approach is a promising option.^{10,17,18} In freshly
89 excreted urine, nitrogen is predominately present as urea; during storage, the microbial enzyme
90 urease hydrolyzes urea to ammonium.¹⁹ Cation adsorption can be used to transfer ammonium
91 from urine to adsorbents (e.g., zeolites,^{10,20} biochar,¹⁰ loess,²¹ ion exchange resins¹⁰). Once
92 saturated, natural adsorbents can be applied as solid fertilizers; ion exchange resins can be
93 regenerated to produce a concentrated ammonia solution for use as fertilizer or disinfectant.

94
95 In a previous study, we compared synthetic and natural adsorbents and demonstrated the
96 recovery of ammonium from urine. The commercial resin Dowex Mac 3 had the highest nitrogen
97 adsorption density (4.23 mmol N g resin⁻¹) and nitrogen recovery efficiency (>99%).¹⁰ While
98 useful for comparing adsorbents and characterizing adsorption isotherms, the batch studies used
99 in the prior study provide limited kinetic information and make it difficult to maintain constant
100 pH,²² which can impact ammonia speciation and sorption. A more appropriate configuration for
101 implementing ion exchange is a flow-through, fixed-bed reactor. In this study, we used
102 continuous-flow column experiments to investigate the impact of operating conditions (e.g., flow
103 rate, concentration) and other design parameters on adsorption and regeneration of ion exchange
104 resins for all three urine macronutrients (N, P, K).

105

106 In addition to nutrients, urine contains trace organic compounds (TrOCs),²³ many of which are
107 contaminants of emerging concern in wastewater treatment because of their deleterious effects
108 on aquatic wildlife²⁴ and uptake by crops.²⁵ Several trace organic compounds are present in urine
109 at concentrations 100-10,000 times that of wastewater.²⁶ While urine separation can effectively
110 reduce input of TrOCs to bulk wastewater, their fate in urine treatment technologies, such as
111 nitrification-distillation,²³ urine storage,²³ electrochemical stripping,⁶ and anion exchange,²⁷ is
112 under investigation. For cation exchange, organic compounds could end up in the urine effluent
113 (which could be discharged to the sewer and go to the wastewater treatment plant), remain in the
114 fertilizer product, or accumulate on the adsorbent. In this study, we investigated the fate of a
115 suite of TrOCs during cation exchange.

116
117 During technology development, systems-level analyses can be used to identify knowledge gaps
118 that merit further study at the laboratory scale. In a previous study, we conducted an economic
119 and environmental assessment of household nitrogen recovery using cation exchange, and found
120 that manufacturing of sulfuric acid (used to regenerate the resin) was the major contributor to
121 energy inputs and greenhouse gas emissions.²⁸ Thus, in the current study we compared
122 alternative regenerants and several metrics of regeneration performance to assess whether these
123 environmental impacts could be reduced.

124
125 The overall goal of this investigation was to characterize continuous-flow recovery of
126 macronutrients from urine using ion exchange. While phosphate recovery by anion exchange has
127 been modeled and optimized in batch and continuous regimes,^{5,16} nitrogen and potassium
128 recovery from urine via cation exchange have only recently been modeled in batch studies.²¹ The

129 specific objectives of this study were to: (i) demonstrate the feasibility of combined recovery of
130 nitrogen, phosphorus, and potassium, (ii) evaluate the effects of operating conditions (flow rate
131 and concentration) on cation adsorption and regeneration, (iii) compare recovery efficiencies of
132 different regenerants, and (iv) determine the fate of several trace organic compounds during
133 cation exchange. The results are promising and provide a basis for evaluating ion exchange for
134 nutrient recovery at the pilot scale.

135

136 **2. MATERIALS AND METHODS**

137 **2.1 Column setup**

138 Columns were constructed from polyvinyl chloride (PVC) plastic (2.54 cm diameter, 16 cm
139 length unless otherwise noted) and operated in continuous upflow mode for both adsorption
140 (synthetic or real urine influent) and regeneration (H_2SO_4 , HCl , HNO_3 , or NaCl influent)
141 experiments. For 16-cm length columns, approximate bed volume was 60 mL. The columns were
142 packed with ion exchange adsorbent and coarse sponges at the ends to retain media. Adsorbents
143 were either Dowex Mac 3 (Sigma Aldrich, St. Louis, MO), a macroporous cation exchange resin,
144 or LayneRT (Layne Christensen Co., The Woodlands, TX), an anion exchange resin modified
145 with ferrous oxide nanoparticles (properties in Table S1). For every experiment, column effluent
146 samples were collected regularly (approximately every 20 minutes) and analyzed for inorganic
147 ions (e.g., ammonium, potassium, and phosphate) via ion chromatography, generating
148 breakthrough curves. All experiments were conducted with analytical grade chemicals at room
149 temperature (23 ± 2 °C).

150

151 **2.2 Combined nutrient recovery**

152 Three treatment trains were compared for combined nutrient recovery: (i) struvite precipitation
153 followed by cation exchange, (ii) anion and cation exchange in series (separate columns), and
154 (iii) simultaneous anion and cation exchange in a mixed-bed column. Ammonium, phosphate,
155 and potassium breakthrough curves were generated for each treatment scheme and compared in
156 terms of bed volumes to 50% breakthrough, slope, and adsorption density. In all setups, real
157 urine was pumped at 4.5 mL min^{-1} . Urine for nutrient recovery was collected from a household
158 urine-diverting toilet in Richmond, California; urine for trace organic analysis was collected
159 from adult volunteers in Berkeley, California. Urine from both sources was stored for several
160 weeks to ensure urea hydrolysis (CPHS protocol 2016-10-9284).

161
162 To recover struvite from hydrolyzed urine, MgCl_2 was added in a 1.1:1 molar ratio of added
163 magnesium to phosphate in 2 L of urine, based on optimal dosing that has been previously
164 reported.¹ The solution was mixed for 10 minutes and settled for 10 minutes; then the
165 supernatant was pumped into another 2-L bottle, and from there into the cation exchange column.
166 For anion and cation exchange in series, hydrolyzed urine was pumped through first the anion
167 and then the cation exchange column. For both configurations (struvite followed by cation
168 exchange and in-series anion and cation exchange), 1.6 L of urine was pumped at 4.5 mL min^{-1}
169 for 6 hours into each of three replicate columns with no recirculation. For the mixed bed, equal
170 masses of LayneRT and Dowex Mac 3 were mixed dry and added to one 32-cm long column to
171 maintain the same bed volume as all other experiments with 16-cm columns. Due to the longer
172 column for mixed-bed recovery, 3.2 L of urine was pumped for 12 hours at 4.5 mL min^{-1} into
173 each of three replicate columns with no recirculation.

174

175 Cation exchange columns with Dowex Mac 3 were pretreated with 10 mL of 1 M borate buffer
176 per gram of resin; LayneRT anion exchange columns were pretreated with 10 mL of pH 12
177 NaOH per gram of resin. Mixed-bed columns were pretreated with 60 mL of pH 12 NaOH per
178 gram resin to avoid borate sorption to the anion exchange resin. Regeneration solutions were
179 based on previous research, which demonstrated regeneration of Dowex Mac 3 and LayneRT
180 resins with varying volumes of 0.122 M H₂SO₄¹⁰ and 2% NaOH/2% NaCl (0.5 M NaOH/0.342
181 M NaCl),²² respectively. Nitrogen and phosphorus recovery efficiencies were compared for these
182 regenerants pumped at 2 mL min⁻¹ through exhausted mixed-bed columns for a total of 300
183 minutes in three setups: NaOH/NaCl only, 150 minutes of H₂SO₄ followed by 150 minutes of
184 NaOH/NaCl, and 150 minutes of NaOH/NaCl followed by 150 minutes of H₂SO₄.

185
186 Effects of operating and design parameters on phosphorus adsorption and elution have been
187 well-characterized in previous studies. For example, phosphate adsorption with hybrid anion
188 exchange resins such as LayneRT has been accurately modeled using a Freundlich isotherm and
189 pseudo-second-order kinetic model;¹⁶ batch adsorption densities have also been determined for
190 influent streams with varying phosphate concentrations.⁵ Regeneration of LayneRT has been
191 optimized to 3.5 bed volumes with 2% NaOH/2% NaCl solution.²⁹ Compared to phosphate,
192 effects of operating and design parameters on cation exchange columns for urine treatment are
193 not well understood and were investigated through additional experiments in this study.

194

195 **2.3 Operating Conditions and Adsorption**

196 Effects of flow rate, influent concentration, and intermittent operation on nitrogen and potassium
197 recovery were investigated through continuous adsorption experiments with synthetic urine and

198 Dowex Mac 3. Synthetic urine was used because of its constant composition (Table S2-S3),
199 whereas real urine composition varies among individuals, times, and regions.³⁰ Based on
200 potential variations in ammonia concentration in real urine, three dilutions of synthetic urine
201 were used: 8000 (undiluted), 5700, and 3600 mg N L⁻¹. 3600 mg N L⁻¹ was indicative of
202 ammonia levels after dilution in NoMix source-separating flush toilets³¹ and 5700 mg N L⁻¹ was
203 chosen as an intermediate concentration. 4.5 mL min⁻¹ was the estimated average urine
204 production rate for a five-person household; this flow rate was halved (2.2 mL min⁻¹) to better
205 represent U.S. conditions (2.5 people household⁻¹),³² and doubled (10 mL min⁻¹) to simulate
206 conditions in which the urine could be collected and then pumped faster than the average
207 generation rate. Each flow rate and concentration condition was conducted in triplicate. Flow
208 rate variations were all conducted with ~1.6 L of undiluted synthetic urine and concentration
209 experiments were performed at constant flow rate (4.5 mL min⁻¹ for 6 hours).

210
211 Intermittent flow was explored because it is more realistic than continuous operation, as toilet
212 use is intermittent. Intermittently run column experiments can also be used to confirm the rate-
213 limiting step of adsorption (e.g., external diffusion, intraparticle diffusion, surface reaction).³³
214 External diffusion refers to transport of the adsorbate from bulk solution to the adsorbent surface,
215 intraparticle diffusion describes transport through the macropores, and the surface reaction is the
216 exchange of ions at adsorption sites.³⁴ Triplicate experiments were performed with synthetic
217 urine in which pumping (4.5 mL min⁻¹) was stopped for 24 hours after 1, 2, 3, and 5 hours of
218 cumulative operation.

219

220 For all column adsorption experiments, adsorption densities were calculated using numerical
221 integration of breakthrough curves (Section S1.1, Equations S1-S2). All adsorption experiments
222 were conducted without recirculation of synthetic urine.

223

224 **2.4 Operating Conditions and Regeneration**

225 Sulfuric acid was previously shown to achieve high recovery efficiency of ammonium from
226 Dowex Mac 3 resin; specifically, 0.122 M H₂SO₄ (0.244 N H₂SO₄) pumped for 2.5 hours at 22.5
227 mL min⁻¹ resulted in >99% nitrogen recovery efficiency.¹⁰ To inform process optimization, we
228 investigated the effects of eluent flow rates, eluent concentrations, and eluent species on
229 regeneration performance metrics.

230

231 We expected low flow rates and high sulfuric acid concentrations to lead to high concentrations
232 of ammonium sulfate eluent. Thus, experiments with 0.5, 1, 3, and 6 M H₂SO₄ were conducted at
233 2 and 4.5 mL min⁻¹ using exhausted resin from synthetic urine adsorption. Next, to determine the
234 effects of operating conditions on regeneration performance metrics, sulfuric acid flow rate and
235 concentration were varied independently and by the same factors (22.5, 10, and 2.25 lower) from
236 the previously established operating parameters that led to 99% nitrogen recovery (0.122
237 M/0.244 N H₂SO₄ at 22.5 mL min⁻¹).¹⁰ To compare process performance for different
238 regenerants that might reduce life-cycle impacts, columns were eluted with equinormal (0.244 N)
239 H₂SO₄, HNO₃, HCl, and NaCl. Nanopure water and tap water were also used as regenerants to
240 determine the extent to which adsorbed ammonia would desorb during resin exposure to water.

241

242 Experimental conditions were compared in terms of ammonium concentration in the fertilizer
243 product, recovery efficiency, bed volumes to 90% elution, and stoichiometric efficiency.
244 Recovery efficiency (Equations S1, S3) and produced ammonium concentration (Equation S7)
245 were calculated by numerical integration. The number of bed volumes to 90% elution was
246 calculated based on cumulative and total area under the elution curve (Equation S4).
247 Stoichiometric efficiency (η_{stoich}) was defined as the proportion of supplied protons (based on
248 commonly available stock concentrations, Table S4) that displaced an ammonium ion on Dowex
249 Mac 3 (Equation 1).

$$250 \quad \eta_{stoich} = \frac{q * W}{Q * t_{elution} * N * C_{regen}} \times 100\% \quad (1)$$

251 In Equation 1, q is adsorption density ($\text{mmol N g resin}^{-1} = \text{meq g resin}^{-1}$), W is resin mass (g
252 resin), Q is flow rate ($\text{mL regenerant solution min}^{-1}$), $t_{elution}$ is time to 90% elution (min, to 90%
253 of total amount eluted), N is normality of regenerant ($\text{meq mmol regenerant}^{-1}$), and C_{regen} is
254 concentration of regenerant ($\text{mmol regenerant L regenerant solution}^{-1}$). Note that as defined, the
255 stoichiometric efficiency is expected to be less than 100% due to the elution of other cations
256 besides ammonium. This definition was chosen because our primary interest was maximizing
257 nitrogen recovery. An alternative definition could account for elution of all cations.

258

259 **2.5 Trace organic contaminants**

260 A suite of 10 trace organic compounds, including antibiotics, antivirals, and beta blockers, was
261 added to real urine before adsorption (Table S5). Compounds were measured in homogenized
262 samples from multiple volunteers according to CPHS protocol 2016-10-9284. Trace organic
263 compounds were quantified with an Agilent 1200 series HPLC (high-performance liquid
264 chromatography) system followed by an Agilent 6460 mass spectrometer (triple quadrupole

265 tandem MS), according to previously published methods for wastewater.³⁵ To determine the fate
266 of urine-relevant TrOCs during ion exchange, concentrations were measured in effluent samples
267 during adsorption with real urine (4.5 mL min⁻¹) and regeneration with 0.122 M sulfuric acid
268 (22.5 mL min⁻¹). Adsorption experiments were run until breakthrough was observed for all
269 compounds ($C_{out}/C_{in} > 0.85$). Based on compound detection limits, the lowest detectable recovery
270 efficiency was 2.8%.

271

272 2.6 Chemical Analysis

273 Ion concentrations (NH₄⁺, Na⁺, K⁺, Li⁺, Mg²⁺, Ca²⁺ and SO₄²⁻, PO₄³⁻, Cl⁻, NO₂⁻, NO₃⁻, F⁻,
274 C₂H₃O₂⁻, Br⁻) were measured via ion chromatography using a Dionex chromatograph (IonPac
275 CS12 column for cations, IonPac AS23 column for anions), as reported previously.¹⁰ Samples
276 were acidified to measure total ammonia nitrogen (TAN) as NH₄⁺. pH was measured with a pH
277 probe and meter (MP220, Mettler Toledo, Columbus, OH).

278

279 2.7 Modeling Breakthrough Curves

280 For every breakthrough curve generated, adsorption density was calculated by numerically
281 integrating breakthrough curves and dividing by adsorbent mass (Equation S2). Breakthrough
282 curves were compared using a two-parameter model that includes bed volumes to 50%
283 breakthrough and slope of the breakthrough curve (Equation 2).³⁴

$$284 \ln \left(\frac{\frac{C_t}{C_0}}{1 - \frac{C_t}{C_0}} \right) = k'(b - \beta) \quad (2)$$

285 In this model, C_t is concentration at time t , C_0 is initial concentration, and b is the number of bed
286 volumes at time t . The two model parameters are k' , the slope of the breakthrough curve, and β ,
287 the number of bed volumes to 50% breakthrough ($C_t/C_0=0.5$). The original model was adapted

288 from breakthrough curves that related absolute concentration and time to breakthrough curves in
289 this study that related relative concentration and bed volumes.

290

291 **2.8 Statistical Analysis**

292 One-way ANOVA and paired t-tests were used to compare calculated adsorption densities and
293 breakthrough model parameters for adsorption breakthrough curves for varying flow rate,
294 influent concentration, and intermittency conditions. A two-tailed significance level of 1%
295 ($p < 0.01$) was used. Parameters (slope k' and bed volumes to 50% breakthrough β) for
296 ammonium breakthrough curves for different combined nitrogen and phosphorus recovery
297 schemes were also compared using one-way ANOVA and paired t-tests.

298

299 **3. RESULTS AND DISCUSSION**

300 **3.1 Combined nitrogen and phosphorus recovery**

301 *3.1.1 Phosphorus Recovery*

302

303 Phosphate was completely removed from hydrolyzed urine during struvite precipitation (Figure
304 S1a). Based on the stoichiometry of nitrogen and phosphorus in struvite ($\text{MgNH}_4\text{PO}_4 \cdot 6\text{H}_2\text{O}$),
305 concentrations of both species were expected to decrease by the same amount (25.9 mM P
306 removed from urine). However, ammonium concentrations only decreased by 84% of the
307 phosphate decrease (Figure S1b), indicating precipitation of phosphate minerals with cations
308 other than ammonium (e.g., hydroxyapatite, $\text{Ca}_5(\text{PO}_4)_3\text{OH}$; potassium struvite formation was
309 likely minimal as the decrease in dissolved potassium concentration was within experimental
310 error).

311

312 Phosphate breakthrough curves for all three treatment trains are shown in Figure 1a. For struvite,
313 phosphate was not detected after precipitation due to complete recovery with MgCl_2 . Although
314 slopes of the mixed-bed and in-series breakthrough curves did not differ significantly, the steeper
315 slope of the in-series curve signaled faster adsorption kinetics (Table S6). Bed volumes to 50%
316 breakthrough were significantly different (7.7 for mixed bed, 10.6 for in series), indicating a
317 reduction in number of available phosphate adsorption sites or slower rate of filling them due to
318 the presence of Dowex Mac 3. Phosphate adsorption densities for mixed-bed and in-series
319 columns were 0.53 and $0.50 \text{ mmol g resin}^{-1}$, respectively, and were not significantly different
320 (Table S6); both were higher than predicted based on expected adsorption densities from a
321 Freundlich isotherm in hydrolyzed urine ($0.255 \text{ mmol P g resin}^{-1}$, Equations S5-S6).¹⁶

322

323 *3.1.2 Nitrogen Recovery*

324 Nitrogen breakthrough curves for struvite supernatant fed to cation exchange, and urine fed to
325 mixed-bed columns, separate columns, and cation exchange alone are presented in Figure 1b.
326 Although struvite supernatant was characterized by more bed volumes to breakthrough and the
327 lowest slope, the lack of statistically significant differences for number of bed volumes to 50%
328 breakthrough and slope for all setups indicated similar ammonium adsorption rates (Table S7).
329 Thus, the presence of LayneRT before cation exchange (in series) and in the same column as
330 Dowex Mac 3 (mixed bed) did not significantly affect kinetics of ammonium adsorption.
331 Ammonium breakthrough was observed latest (largest β) for struvite supernatant due to the
332 removal of approximately 9% of ammonium during struvite precipitation and lower influent
333 urine ammonium concentrations. Similarly, adsorption density for struvite supernatant was lower
334 than all other setups, although only significantly lower than the mixed-bed column (Table S7).

335

336 *3.1.3 Potassium Recovery*

337 The molar adsorption density for potassium in synthetic urine (0.3-0.4 mmol K g resin⁻¹) was
338 more than ten times lower than the nitrogen adsorption density (4.23 mmol N g resin⁻¹). Both the
339 tenfold lower concentration of potassium in urine and the selectivity of Dowex Mac 3 for NH₄⁺
340 contributed to low potassium adsorption. Potassium also began to break through the column
341 ($C_{out}/C_{in}>0$) at fewer bed volumes than nitrogen (Figure S2). Thus, to achieve higher potassium
342 recovery, it should be removed in a separate column from nitrogen or with an adsorbent other
343 than Dowex Mac 3. Bed volumes to 50% elution, slopes of breakthrough curves, and adsorption
344 densities did not differ significantly between setups, indicating that potassium adsorption was not
345 affected by phosphate recovery (Table S8). Potassium has not been a priority for nutrient
346 recovery because it has not been shown to contribute to eutrophication, it is less abundant in
347 urine than nitrogen, and it has a lower specific value than phosphorus (1.5 USD kg P⁻¹, 0.7-1
348 USD kg K⁻¹);³⁶ thus potassium recovery was not optimized in this study. Future work could
349 optimize potassium recovery by potassium struvite precipitation or by cation exchange after
350 nitrogen recovery to enhance the value of combined nutrient fertilizers derived from urine.

351

352 *3.1.4 Considerations for implementation*

353 Molar nitrogen adsorption densities were up to an order of magnitude higher than phosphorus
354 adsorption densities due to the lower adsorption capacity of LayneRT (phosphate) compared to
355 Dowex Mac 3 (ammonium). Accounting for differences in adsorption density and concentration
356 in urine, the treatment of 1 L of urine would require 106 g LayneRT and 50 g Dowex Mac 3.
357 Thus, mixed-bed columns should have roughly twice as much LayneRT as Dowex Mac 3, and

358 for separate columns the cation exchange column could contain half the resin mass as the anion
359 exchange column.

360

361 While separate regenerants can be used for each resin type for columns in series, regeneration of
362 a mixed-bed column exposes both anion and cation exchange resins to any regenerant used. For
363 mixed-bed regeneration, ammonium recovery efficiencies were higher than phosphate recovery
364 efficiencies for all regenerants tested (50-60% for N and 20-30% for P, Figure S3). Desorption of
365 ammonium occurred faster than phosphate desorption due to the more tightly bound Lewis acid-
366 base interactions between phosphate and the anion exchange resin.²² Further decreasing flow rate
367 (below 2 mL min⁻¹, thus increasing hydraulic residence time) could potentially enhance
368 phosphate recovery efficiency. 2% NaOH/2% NaCl exhibited the highest recovery efficiencies
369 for both phosphorus and nitrogen (Figure S3). Compared to NaOH/NaCl, eluting with sulfuric
370 acid first halved the phosphorus recovery efficiency, and eluting with sodium chloride/hydroxide
371 first reduced ammonium recovery efficiency by 10% (Figure S3). Thus, exposing LayneRT to a
372 pH far below its operating range (5.5-8.5) negatively affected phosphate desorption more than
373 sodium affected ammonium desorption.

374

375 Based on our results, operating cation and anion columns separately (rather than in a mixed bed)
376 appears more promising for maximizing the recovery efficiency of nitrogen, potassium, and
377 phosphorus. In addition, recovering the nutrients separately would allow them to be recombined
378 in different ratios to produce tailored fertilizers. Also, phosphorus recovery could occur through
379 struvite precipitation (stored urine) or anion exchange (fresh or stored urine). Recovering
380 phosphate via anion exchange in fresh urine would reduce the precipitation of phosphate

381 minerals such as struvite and hydroxyapatite because of low ammonia concentrations and the
382 lower pH of fresh urine (6 vs. 9 in stored urine).⁵ Urea hydrolysis could be accelerated by adding
383 urease enzyme or optimizing conditions for microbial hydrolysis (e.g., fixed biofilm column,
384 increasing temperature). For example, phosphorus precipitation from fresh urine, urea hydrolysis
385 in a fixed biofilm column, and ammonium and potassium adsorption in separate cation exchange
386 columns operated in series could be an effective treatment scheme.

387

388 **3.2 Effects of operating conditions on adsorption**

389 The number of bed volumes to breakthrough varied inversely with total ammonia concentration
390 in influent synthetic urine and was significantly different for each concentration (Figure 2a). This
391 trend was expected given a fixed number of sites available per gram of resin, which were
392 occupied in fewer bed volumes when more ammonium ions were present (higher concentration).
393 The slope of the breakthrough curves was not significantly different for varying concentrations.
394 Adsorption densities did not differ significantly (Figure S4), which was expected given that this
395 range of the adsorption isotherm is relatively flat.¹⁰

396

397 Variations in flow rate within the range tested did not have a significant impact on bed volumes
398 to breakthrough nor slope of the breakthrough curve (Figure 2b). Adsorption densities for
399 varying flow rates were not significantly different (Figure 2c). Because breakthrough curve slope
400 was not affected by increasing flow rate from 2.2 to 10 mL min⁻¹ (and thus the rate at which
401 ammonium is supplied), transport through the liquid film could be excluded as the rate-limiting
402 step of the adsorption process within this range.³³

403

404 Intermittent flow of urine led to similar adsorption density as continuous flow (no significant
405 difference). After each 24-hr rest period, effluent ammonium concentrations decreased (Figure
406 2d). This decrease could have been due to microbial oxidation or sorption. Based on low NO_2^-
407 and NO_3^- concentrations in the column effluent (below detection limit of 1 mg L^{-1}), additional
408 ammonium adsorption was identified as the predominant mechanism. Gaseous products (e.g., N_2 ,
409 NO , N_2O) could have been formed from microbial oxidation, but no bubbles were observed
410 despite N_2 , NO , and N_2O being water-insoluble gases ($K_{\text{H}} \leq 2.5 \times 10^{-2} \text{ M atm}^{-1}$,³⁷ Table S9).
411 Ammonia adsorption during quiescence demonstrated that intraparticle diffusion (i.e. transport
412 through resin macropores) was likely the rate-limiting step of ammonia removal via ion
413 exchange.³³ Ammonia concentrations no longer decreased once the resin was exhausted (i.e.,
414 between day 4 and day 5).

415
416 For potassium adsorption, the only significant differences were between the number of bed
417 volumes to 50% breakthrough for the most dilute influent concentration and the other
418 concentrations tested (Figure S2). Adsorption densities were not significantly different and no
419 clear trend was observed (Figure S6). Potassium emerged from the column in fewer bed volumes
420 than ammonium for all conditions tested.

421

422 **3.3 Effects of operating conditions on regeneration**

423 In addition to having a high recovery of the target nutrient(s), an optimal regenerant would have
424 few bed volumes to elution and a high stoichiometric efficiency. The last parameter minimizes
425 the volume of regenerant required for elution, which is important because our previous analysis
426 identified that the acid regenerant dominated the life-cycle costs, embedded energy, and

427 greenhouse gas emissions of the entire process.²⁸ Also, for ion exchange to be a viable process
428 for nutrient recovery from urine, nutrients in the final product must be significantly more
429 concentrated than in the original urine.

430

431 The impact of different operating conditions on the elution step was investigated using
432 ammonium as the target nutrient. The first objective was to determine if up-concentration could
433 be achieved, i.e., was the nitrogen concentration in the ammonium sulfate eluent higher than in
434 the influent urine. We estimated that the theoretical minimum number of bed volumes required
435 to up-concentrate ammonium from urine was 8, assuming the urine contained 5 g N L⁻¹
436 (Equation S9). Experimentally, we achieved up-concentration using 0.5 to 6 M H₂SO₄ (Table 1).
437 A more concentrated product was achieved with stronger acid, with a final ammonium sulfate
438 product containing 22 g N L⁻¹, which is 25% of common (NH₄)₂SO₄ liquid fertilizers available
439 on the market (Equations S7-S8).^{38,39} Instantaneous ammonium concentrations were as high as
440 60 g N L⁻¹ (Figure S7a). Bed volumes to elution were minimized to 2.78 bed volumes using 6 M
441 H₂SO₄, whereas 5.15 bed volumes were required when 0.5 M H₂SO₄ was used. However, the
442 stoichiometric efficiency was lower for the higher concentration eluent: 19% compared to 83.5%
443 for 6 and 0.5 M H₂SO₄, respectively (Table 1). Thus, there was a trade-off between up-
444 concentrating the nitrogen and using the acid eluent efficiently.

445

446 Increasing the regeneration flowrate from 2 to 4.5 mL min⁻¹ did not appear to impact elution
447 performance (Figure S7b). For all four H₂SO₄ concentrations, most regeneration parameters
448 (e.g., recovery efficiency, final ammonium concentration) differed by less than 15% at 2 and 4.5
449 mL min⁻¹ (Table 1, Table S10). Similar concentration trends were observed at both flow rates, as

450 higher H₂SO₄ concentrations led to lower bed volumes to elution, lower stoichiometric
451 efficiencies, and higher final ammonium concentrations. Nonetheless, we wanted to explore the
452 impacts of flow rate and concentration of acid regeneration over a wider range of conditions.
453 Based on preliminary experiments, repeatable samples could not be collected quickly enough to
454 generate reliable elution curves at high sulfuric acid concentrations and higher flow rates (>4.5
455 mL min⁻¹). Thus, we compared elution at flow rates and concentrations that allowed us to
456 explore these variables but were not effective for up-concentration.

457
458 Elution curves for varying flow rate and sulfuric acid concentration are shown in Figure S5.
459 Stoichiometric efficiency varied inversely with flow rate and sulfuric acid concentration (Figure
460 3). Nitrogen recovery efficiency was consistently above 90%, with the exception of the 5.42 mM
461 sulfuric acid, the lowest concentration tested (Figure S8). Although increasing flow rate did not
462 have a significant effect on bed volumes to 90% elution, increasing concentration drastically
463 reduced bed volumes to elution (Figure 3a). Regenerant concentration had a larger effect (higher
464 absolute value of slope) than flow rate on stoichiometric efficiency and bed volumes required for
465 both nitrogen (Figure 3) and potassium (Figure S9). Based on these results, proton activity was
466 the predominant operating parameter influencing the volume of acid required for elution. The
467 lack of effect from flow rate on bed volumes to elution indicated that proton loading rates for the
468 flow rates tested were sufficiently high to desorb ammonium. For potassium, most recovery
469 efficiencies were above 90% (Figure S10).

470
471 While up-concentration is desirable, more acid was required for concentrating ammonium during
472 elution, demonstrating that it was not possible to maximize both product concentration and

473 stoichiometric efficiency. To overcome this limitation, future work could explore re-using the
474 ammonium sulfate eluent for multiple elutions to produce more concentrated product and
475 increase the stoichiometric efficiency. Alternatively, elution could be optimized for
476 stoichiometric efficiency, and a separate step, such as reverse osmosis, could be added to
477 concentrate the eluent.

478

479 **3.4 Comparing regenerants**

480 Bed volumes to 90% elution, stoichiometric efficiency, and nitrogen recovery efficiency for
481 equinormal (0.244 N) HNO₃, HCl, NaCl, and H₂SO₄ are compared in Table 2 (elution curves in
482 Figure S11). Of the regenerants tested, sulfuric acid exhibited the lowest number of bed volumes
483 to elution and stoichiometric efficiency, indicating the most efficient use of regenerant. The only
484 significant differences between performance metrics for different regenerants were the nitrogen
485 recovery efficiency of NaCl (77%) with all other regenerants (all approximately 100%). NaCl
486 had a lower nitrogen recovery efficiency because of the lower affinity of Dowex Mac 3 for
487 sodium ions compared to protons and ammonium.¹⁰ This low performance of NaCl regeneration
488 may potentially be mitigated by using more concentrated NaCl regenerants. With NaCl, the Na⁺
489 sorbed during column regeneration would desorb during subsequent urine treatment, increasing
490 the salinity of the urine effluent. If this stream is disposed to the sewer, it could be a
491 disadvantage for treatment plants that discharge to inland freshwater or if the water is reused; for
492 ocean discharge, the additional salinity is likely not an issue.

493

494 For potassium recovery with Dowex Mac 3, no significant differences in elution metrics were
495 observed. At most 8% of protons contributed to potassium desorption for all regenerants, which

496 was expected given the tenfold lower adsorption density of potassium compared to ammonium.
497 Similar to nitrogen results, all three acid regenerants exhibited potassium recovery efficiencies of
498 at least 100% while NaCl was only 87%; sulfuric acid had the lowest number of bed volumes to
499 90% potassium elution (Table S11).

500

501 To evaluate the potential for desorption if the column is exposed to water, nanopure water and
502 tap water were used as regenerants on ammonium-loaded Dowex Mac 3 resin. Based on elution
503 curves (Figure S12), only 6.9% (nanopure) and 8.9% (tap) of sorbed ammonium was desorbed
504 during 2.7 L of water flow. The low proton concentration in these waters can explain the
505 unfavorable desorption of ammonium. Low levels of elution with water indicate that desorption
506 of ammonium due to exposure to very dilute urine streams, flush water, or water used for
507 cleaning is not a major impediment.

508

509 **3.5 Fate of indicator trace organics**

510 Trace organics could adsorb to Dowex Mac 3 via electrostatic or van der Waals interactions. As
511 expected, only trace organic contaminants that were positively charged at stored urine pH (~9.1)
512 were adsorbed (Figure 4a), indicating electrostatic interactions as the primary mechanism.
513 Neutral and negatively charged compounds of similar size to adsorbed compounds were not
514 adsorbed to Dowex Mac 3, including sulfamethoxazole, acetaminophen, acyclovir, and
515 emitricitabine. Adsorbed compounds were identified as positively charged based on comparing
516 stored urine pH to published pK_a values (Table S5), with two exceptions: abacavir and
517 trimethoprim (Figure 4a). Although abacavir has a published pK_a of 5.01, it is regarded as a
518 monoacidic base because of delocalized positive charge in the heterocycle.⁴⁰ Similarly,

519 trimethoprim has a pK_a of 7.4, which would indicate neutral charge at pH 9 in stored urine.
520 However, trimethoprim has been particularly well-removed by synthetic macroporous resins and
521 zeolites;⁴¹ it has also been suggested to be positively charged when bound to enzymes like
522 dihydrofolate reductases.⁴² These enzymes are required for production of purines and some
523 amino acids, and are thus ubiquitous in bacterial cells present in stored urine ($\sim 5 \times 10^8$ cells mL⁻¹).³
524

525
526 TrOC adsorption onto anion exchange resins has been measured and modeled for several non-
527 steroidal anti-inflammatory drugs (e.g., diclofenac, naproxen).²⁷ Acetaminophen (also called
528 paracetamol) was the only compound also monitored in this study, and did not appreciably
529 adsorb to anion nor cation exchange resins due to only 40% being negatively ionized (60%
530 neutral) at pH 9. For anion exchange resins, electrostatic interactions were responsible for TrOC
531 adsorption densities while selectivity was a function of hydrophobicity.²⁷ Based on only
532 positively charged organic compounds adsorbing to Dowex Mac 3, adsorption density and thus
533 removal efficiency during adsorption were functions of electrostatic interactions. Given the
534 similar polymeric backbones of anion and cation exchange resins, selectivity is also expected to
535 be a function of hydrophobicity and van der Waals interactions for cation exchange resins. In
536 future work similar suites of prevalent trace organic compounds could be applied to both resin
537 types.

538
539 Elution suited for nitrogen recovery was used with TrOC-loaded resin to determine TrOC
540 concentrations in produced ammonium sulfate and recovery efficiencies for trace organics. Only
541 beta blockers (atenolol and metoprolol) were eluted (Figure 4b), and at less than 10%

542 efficiencies. This finding indicates that the majority of atenolol and metoprolol, as well as
543 compounds that were adsorbed but not eluted (carbamazepine, zidovudine, abacavir, and
544 trimethoprim), will continue to accumulate on Dowex Mac 3 over multiple adsorption-
545 regeneration cycles. Atenolol ($0.046 \pm 0.013 \mu\text{g L}^{-1}$) and metoprolol ($0.077 \pm 0.028 \mu\text{g L}^{-1}$) were
546 also the only compounds at detectable levels in the ammonium sulfate product.

547
548 Many pharmaceuticals present in urine are contaminants of emerging concern that should be
549 treated before discharge to avoid harming aquatic organisms. Based on many TrOCs passing
550 through cation exchange columns, pre-or post-treatment for TrOC removal in urine will be
551 required. For the compounds that accumulate on Dowex Mac 3, regeneration may be required
552 and has been demonstrated for anion exchange resins with 5% (m/m) NaCl with equal volumes
553 of water and methanol.²⁷ Atenolol and metoprolol in the ammonium sulfate product should also
554 be monitored for environmental impacts. When biosolids containing atenolol were applied to
555 corn, carrot, and potato crops, atenolol was detected in the $0.5\text{-}1 \text{ ng L}^{-1}$ range in the plants, which
556 was not considered significant uptake.⁴³ Metoprolol may behave similarly, but has not been
557 measured during field trials. While these data indicate that urine-derived ammonium sulfate
558 concentrate does not contain biologically significant pharmaceutical levels, future work can more
559 robustly answer this question for additional compounds to ensure urine-derived fertilizers do not
560 lead to additional uptake of pharmaceuticals by crops.

561 562 **4. Conclusions**

563 In this study, the effects of operating parameters of adsorption and regeneration on system
564 performance were investigated for nutrient recovery via ion exchange. Based on previous life-
565 cycle analysis that indicated sulfuric acid manufacturing contributes significantly to energy use

566 and greenhouse gas emissions,²⁸ efficacies of alternative regenerants were compared. Removal
567 of trace organics during cation exchange was determined, and treatment schemes for nitrogen
568 and phosphorus recovery were compared. Overall, these findings contribute to an improved
569 understanding of continuous-flow nitrogen recovery via ion exchange. The major implications of
570 this work for implementation were:

- 571 • Several configurations for recovery of phosphorus, nitrogen, and potassium were
572 identified, either by operating anion and cation exchange in series or by integrating
573 struvite precipitation with cation exchange.
- 574 • Ammonium recovery from urine can be performed intermittently and regenerated
575 periodically to produce ammonium sulfate concentrate.
- 576 • Acidic regenerants performed better than sodium chloride and avoid brine generation.
- 577 • Trace organics that are positively charged at pH 9 were co-adsorbed with ammonium.
578 Adsorbed compounds were not substantially eluted into the ammonium sulfate product,
579 but may accumulate on resin over several adsorption-regeneration cycles.

580 Based on these conclusions, the primary barriers to adoption relate to implementation and can be
581 better understood at pilot scale. To advance ion exchange-based nutrient recovery from urine,
582 future work could more comprehensively analyze the fate of additional trace organic compounds
583 and optimize nitrogen recovery in terms of product concentration and efficient regenerant use.

584 Based on a vision for selective nutrient recovery and production of customized fertilizers of any
585 desired NPK (nitrogen: phosphorus: potassium) ratio, additional adsorbents for phosphate and
586 potassium recovery could be further explored and integrated into a complete treatment train for
587 nutrient recovery from source-separated urine.

588

589 **ASSOCIATED CONTENT**

590 The Supporting Information (SI) contains equations for breakthrough curve parameters,
591 composition of synthetic urine and properties of trace organic contaminants, and adsorption and
592 elution curves. This information is available free of charge via the Internet.

593

594 **AUTHOR INFORMATION**

595 Corresponding author (K.L.N.):

596 Phone: 510-643-5023; e-mail: karanelson@berkeley.edu

597 **Notes**

598 The authors declare no competing financial interests.

599

600 **ACKNOWLEDGEMENTS**

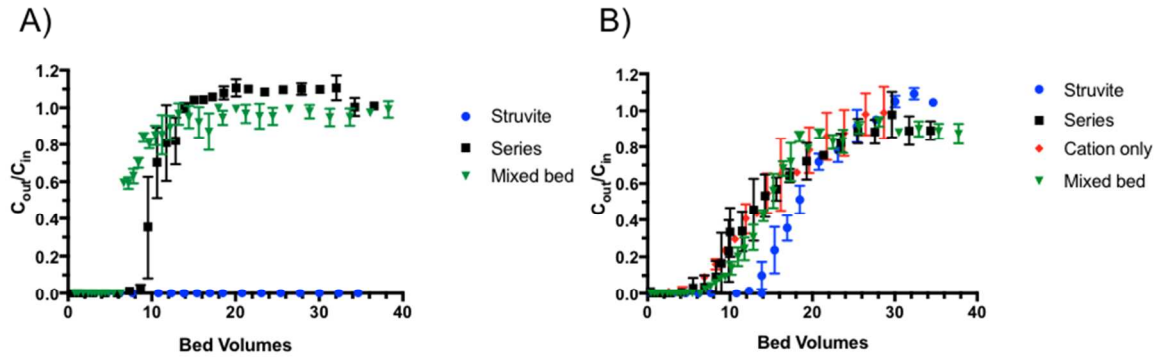
601 W.A.T. and K.L.N. acknowledge research funding from the National Science Foundation (NSF)
602 through the ReNUWIt Engineering Research Center (<http://renuwit.org>; NSF Grant No. CBET-
603 0853512). W.A.T. was also supported by an NSF Graduate Research Fellowship (NSF Grant No.
604 DGE 1106400) and a Ford Foundation Fellowship. We would also like to thank Dr. Eberhard
605 Morgenroth for supporting M.W. during her research exchange at UC Berkeley.

606 **References**

- 607 1 Etter, E. Tilley, R. Khadka and K. M. Udert, *Water Res.*, 2011, **45**, 852–862.
- 608 2 T. A. Larsen and W. Gujer, *Water Sci. Technol.*, 1996, **34**, 87–94.
- 609 3 R. H. Lahr, H. E. Goetsch, S. J. Haig, A. Noe-Hays, N. G. Love, D. S. Aga, C. B. Bott, B.
- 610 Foxman, J. Jimenez, T. Luo, K. Nace, K. Ramadugu and K. R. Wigginton, *Environ. Sci.*
- 611 *Technol.*, 2016, **50**, 11619–11626.
- 612 4 L. Decrey, K. M. Udert, E. Tilley, B. M. Pecson and T. Kohn, *Water Res.*, 2011, **45**, 4960–
- 613 4972.
- 614 5 J. A. O’Neal and T. H. Boyer, *Water Res.*, 2013, **47**, 5003–5017.
- 615 6 W. A. Tarpeh, J. M. Barazesh, T. Y. Cath and K. L. Nelson, *Environ. Sci. Technol.*, 2018, **52**,
- 616 1453–1460.
- 617 7 M. E. R. Christiaens, S. Gildemyn, S. Matassa, T. Ysebaert, J. De Vrieze and K. Rabaey,
- 618 *Environ. Sci. Technol.*, 2017, **51**, 13143–13150.
- 619 8 P. Ledezma, P. Kuntke, C. J. N. Buisman, J. Keller and S. Freguia, *Trends Biotechnol.*, 2015,
- 620 **33**, 214–220.
- 621 9 X. Chen, Y. Gao, D. Hou, H. Ma, L. Lu, D. Sun, X. Zhang, P. Liang, X. Huang and Z. J. Ren,
- 622 *Environ. Sci. Technol. Lett.*, , DOI:10.1021/acs.estlett.7b00168.
- 623 10 W. A. Tarpeh, K. M. Udert and K. L. Nelson, *Environ. Sci. Technol.*, 2017, **51**, 2373–2381.
- 624 11 Z. Ganrot, A. Slivka and G. Dave, *CLEAN – Soil Air Water*, 2008, **36**, 45–52.
- 625 12 N. P. Kocatürk and B. B. Baykal, *CLEAN–Soil Air Water*, 2012, **40**, 538–544.
- 626 13 A. Casadellà, P. Kuntke, O. Schaetzle and K. Loos, *Water Res.*, 2016, **90**, 62–70.
- 627 14 A. Hug and K. M. Udert, *Water Res.*, 2013, **47**, 289–299.
- 628 15 A. Triger, J.-S. Pic and C. Cabassud, *Water Res.*, 2012, **46**, 6084–6094.
- 629 16 A. Sendrowski and T. H. Boyer, *Desalination*, 2013, **322**, 104–112.
- 630 17 B. Beler-Baykal and S. Cinar-Engin, *J. Water Supply Res. Technol.*, 2007, **56**, 541.
- 631 18 D. Karadag, S. Tok, E. Akgul, M. Turan, M. Ozturk and A. Demir, *J. Hazard. Mater.*, 2008,
- 632 **153**, 60–66.
- 633 19 K. M. Udert, T. A. Larsen and W. Gujer, *Water Res.*, 2003, **37**, 2667–2677.
- 634 20 B. Beler-Baykal, A. D. Allar and S. Bayram, *Water Sci. Technol. J. Int. Assoc. Water Pollut.*
- 635 *Res.*, 2011, **63**, 811–817.
- 636 21 S. Jiang, X. Wang, S. Yang and H. Shi, *Environ. Sci. Pollut. Res.*, 2016, **23**, 2628–2639.
- 637 22 L. M. Blaney, S. Cinar and A. K. SenGupta, *Water Res.*, 2007, **41**, 1603–1613.
- 638 23 H. N. Bischel, B. D. Özel Duygan, L. Strande, C. S. McArdell, K. M. Udert and T. Kohn,
- 639 *Water Res.*, 2015, **85**, 57–65.
- 640 24 N. Bolong, A. F. Ismail, M. R. Salim and T. Matsuura, *Desalination*, 2009, **239**, 229–246.
- 641 25 A. J. Hamilton, F. Stagnitti, X. Xiong, S. L. Kreidl, K. K. Benke and P. Maher, *Vadose Zone*
- 642 *J.*, 2007, **6**, 823–840.
- 643 26 R. Zhang, P. Sun, T. H. Boyer, L. Zhao and C.-H. Huang, *Environ. Sci. Technol.*, 2015, **49**,
- 644 3056–3066.
- 645 27 K. A. Landry, P. Sun, C.-H. Huang and T. H. Boyer, *Water Res.*, 2015, **68**, 510–521.
- 646 28 O. Kavvada, W. A. Tarpeh, A. Horvath and K. L. Nelson, *Environ. Sci. Technol.*, 2017, **51**,
- 647 12061–12071.
- 648 29 A. T. Williams, D. H. Zitomer and B. K. Mayer, *Environ. Sci. Water Res. Technol.*, 2015, **1**,
- 649 832–838.

- 650 30C. Rose, A. Parker, B. Jefferson and E. Cartmell, *Crit. Rev. Environ. Sci. Technol.*, 2015, **45**,
651 1827–1879.
- 652 31L. Rossi, J. Lienert and T. A. Larsen, *J. Environ. Manage.*, 2009, **90**, 1909–1917.
- 653 32 *Families and Living Arrangements*, U.S. Census Bureau.
- 654 33P. Li and A. K. SenGupta, *React. Funct. Polym.*, 2000, **44**, 273–287.
- 655 34M. S. Onyango, T. Y. Leswifi, A. Ochieng, D. Kuchar, F. O. Otieno and H. Matsuda, *Ind. Eng.*
656 *Chem. Res.*, 2009, **48**, 931–937.
- 657 35J. T. Jasper, Z. L. Jones, J. O. Sharp and D. L. Sedlak, *Environ. Sci. Technol.*, 2014, **48**, 5136–
658 5144.
- 659 36T. A. Larsen, K. M. Udert and J. Lienert, Eds., *Source Separation and Decentralization for*
660 *Wastewater Management*, IWA Publishing, 1st edn., 2013.
- 661 37R. Sander, *Atmos Chem Phys*, 2015, **15**, 4399–4981.
- 662 38O. L. Vargas and D. R. Bryla, *HortScience*, 2015, **50**, 479–485.
- 663 39 *Liquid Fertilizer Formulation Guide*, AdvanSix Inc., 2016.
- 664 40M. S. Goizman, T. É. Balayants, A. A. Kamalova, A. O. Popova, A. A. Korlyukov, K. Y.
665 Suponitskii, A. S. Trifilenkov, S. K. Papikyan, N. L. Shimanovskii, S. A. Zaitsev, A. S.
666 Berlyand and E. V. Degterev, *Pharm. Chem. J.*, 2015, **49**, 65–72.
- 667 41D. R. U. Knappe, A. Rossner, S. A. Snyder and C. Strickland, *Alternative Adsorbents for the*
668 *Removal of Polar Organic Contaminants*, American Water Works Association, 2007.
- 669 42G. Roberts, J. Feeney, A. Burgen and S. Daluge, , DOI:10.1016/0014-5793(81)80893-9.
- 670 43L. Sabourin, P. Duenk, S. Bonte-Gelok, M. Payne, D. R. Lapen and E. Topp, *Sci. Total*
671 *Environ.*, 2012, **431**, 233–236.
672
673

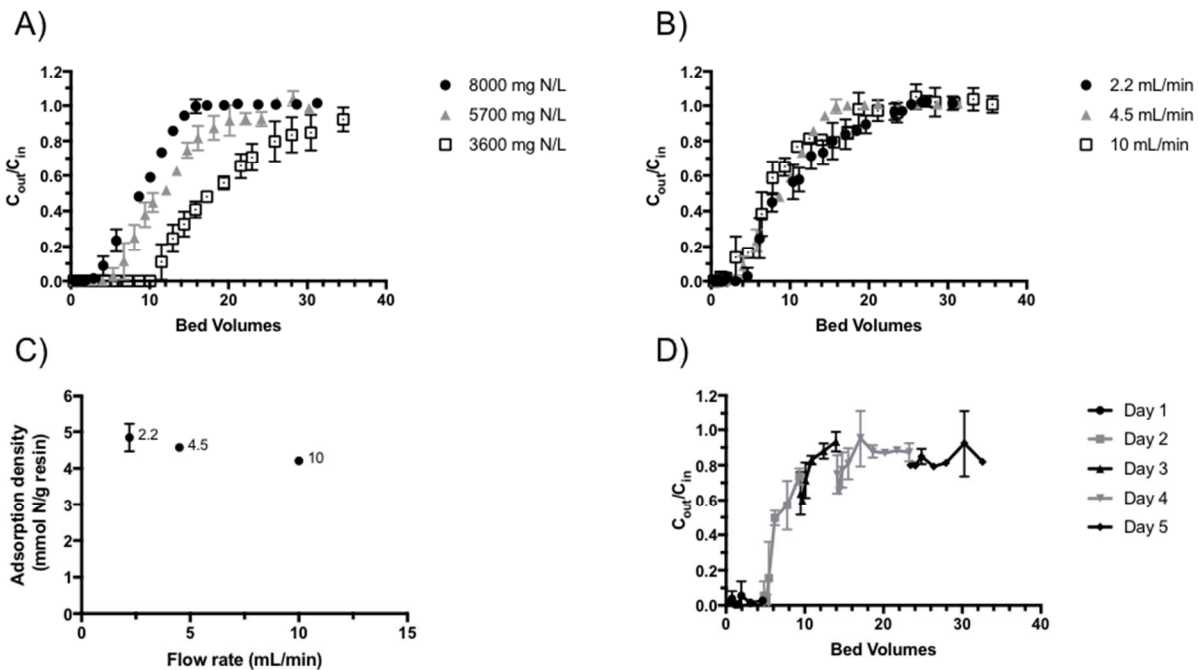
674 FIGURES



675

676 **Figure 1.** Breakthrough curves for varying treatment trains for (a) phosphorus as phosphate and
 677 (b) nitrogen as ammonium.

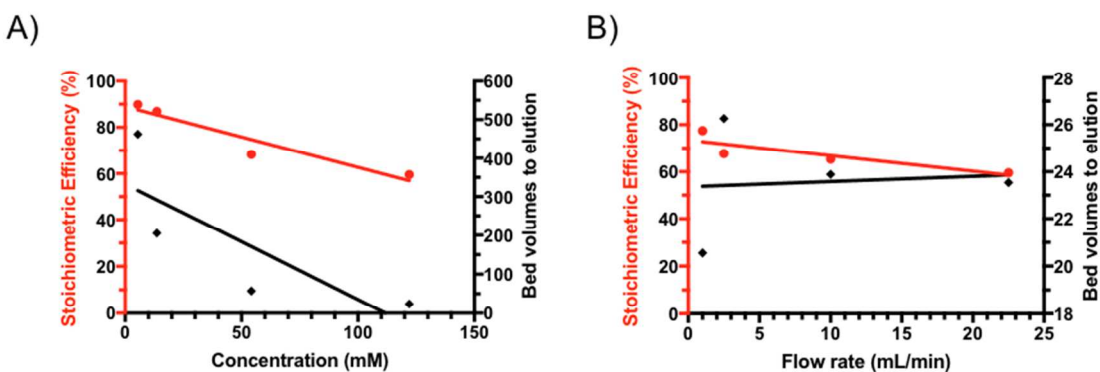
678



679

680 **Figure 2.** Ammonium breakthrough curves with synthetic urine influent for (a) varying influent
 681 TAN concentration and (b) varying flow rate. Panel (c) shows adsorption densities for varying
 682 flow rate with undiluted synthetic urine (8000 mg N L^{-1}), and point labels are flow rates. Panel

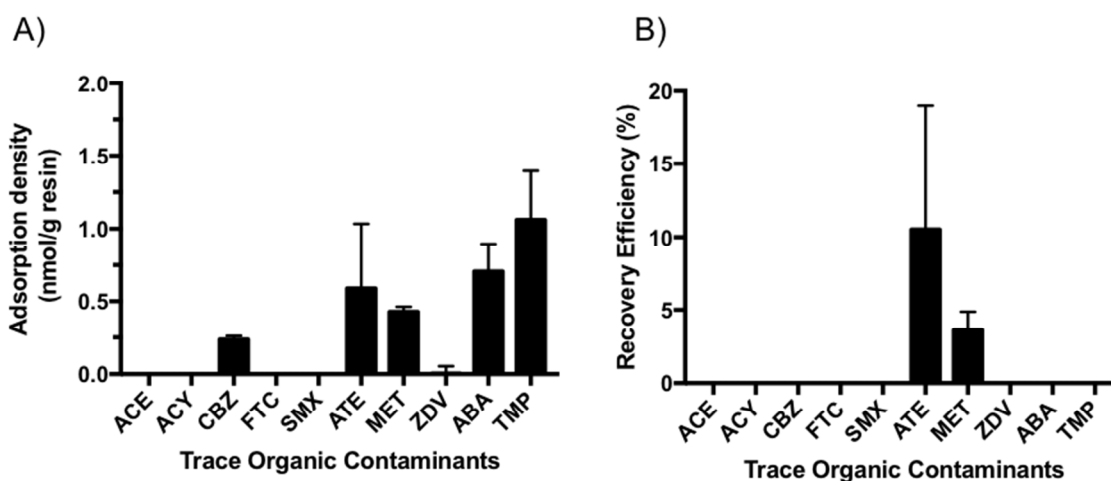
683 (d) shows ammonium breakthrough for intermittent operation. Error bars represent \pm one
 684 standard deviation for experimental triplicates. Error bars not shown are smaller than symbol.



685
 686 **Figure 3.** Sulfuric acid use efficiency compared to stoichiometric exchange for ammonium
 687 elution and column regeneration with (a) varying concentration (flow rate constant at 22.5 mL
 688 min^{-1}) and (b) varying flow rate (concentration constant at 122 mM H_2SO_4). Linear regression
 689 lines show slope of each correlation. Resin was exhausted during adsorption with synthetic urine.

690

691



692
 693 **Figure 4.** (a) Adsorption density and (b) recovery efficiency of trace organic contaminants with
 694 cation exchange resin Dowex Mac 3. Compound abbreviations are in Table S5.

695 **TABLES**

696

697 **Table 1.** Ammonium recovery efficiencies, stoichiometric efficiencies, final eluent
 698 concentrations, and bed volumes to 90% elution for elution experiments at high concentration
 699 and 2 mL min⁻¹. Resin was exhausted during adsorption with synthetic urine. TAN is total
 700 ammonia nitrogen.

701

H ₂ SO ₄ Concentration (M)	Bed volumes to 90% elution	Stoichiometric Efficiency (%)	Recovery Efficiency (%)	Final Eluent TAN (g N L ⁻¹)
0.5	5.15	83.5	90.7	7.87
1	5.06	54.4	88.4	7.21
3	3.02	33.3	81.4	22.3
6	2.78	19.1	101	22.2

702

703

704 **Table 2.** Ammonium recovery efficiencies, stoichiometric efficiencies, and bed volumes to 90%
 705 elution for triplicate elution experiments with various regenerants. Resin was exhausted during
 706 adsorption with synthetic urine. Error values denote standard error of the mean (SEM).

707

	Bed volumes to 90% elution	Stoichiometric Efficiency (%)	Recovery Efficiency (%)
HNO ₃	21.9 ± 1.76	95.3 ± 2.4	104 ± 1.8
HCl	23.2 ± 0.87	101 ± 3.4	102 ± 4.2
NaCl	28.9 ± 2.81	85.9 ± 10.7	77.4 ± 5.5
H ₂ SO ₄	20.0 ± 2.19	107 ± 16.8	99.3 ± 0.3*

708

*experimental duplicate

709

710

711

712

